

<https://doi.org/10.37434/tpwj2021.10.02>

STRUCTURAL INHOMOGENEITY IN WELDED JOINTS OF HEAT-RESISTANT STEELS OF CHROMIUM-MOLYBDENUM-VANADIUM SYSTEM WITH DIFFERENT CHROMIUM CONTENT

M.O. Nimko, V.Yu. Skulskyi, A.R. Gavryk, S.I. Moravetskyi and I.G. Osypenko

E.O. Paton Electric Welding Institute of the NASU
11 Kazymyr Malevych Str., 03150, Kyiv, Ukraine

ABSTRACT

Welded joints of dissimilar steels are widely used in different assemblies of the steam-water mixture loop in electric power plants. Difference in alloying by chromium and other carbide-forming elements results in carbon migration from the lower alloyed to the higher alloyed steel in such joints after tempering and in high-temperature service. Decarbonization in the HAZ near-weld zone of the lower alloyed steel can lead to formation of defects and subsequent failures. In this work we studied the influence of the type of 15Kh2M2FBS steel joint (single-pass, multipass), made using electrodes with 9 % Cr, on the nature of formation and development of structural inhomogeneity in the HAZ at high-temperature annealing. It is shown that depending on joint type, development of ferrite interlayer takes place in different zones of the HAZ: in the normalized zone and in the zone of intercritical temperatures A_{C1} – A_{C3} at a distance from the fusion line at single-pass welding; and in the near-weld zone through the HAZ coarse-grained region at multipass welding. Proceeding from the features of decarbonization on the surfaces of butt joints and near the fusion line, a scheme was proposed, that allows explaining the nature of development of structural inhomogeneity in the multipass joint of dissimilar steels.

KEY WORDS: carbon diffusion, dissimilar steel joints, heat-affected zone, decarbonized interlayer

The main thermodynamic cycle of thermal power plants used in modern heat power engineering, is the Rankine cycle with steam overheating. To implement this thermal cycle different sections of steam-water loop at the power plant should have different parameters of working medium temperature and pressure. In order to lower the cost of power plant construction, the sections with lower steam parameters are made from low-alloy bainitic steels with 0.5–2.25 % Cr (wall-mounted screen boiler pipes; up to 600 °C temperatures) and martensitic steels with 9–12 % Cr (upper pipe sections of wall-mounted screens of the boiler, headers, main steam lines; up to 625–630 °C temperatures), while sections with higher steam parameters are made from more expensive austenitic steels (superheater coils; up to 660–680 °C) [1]. To realize a closed steam-water loop all these sections are connected to each other by welding, forming a dissimilar steel joints.

In such joints a decarbonized interlayer forms on the side of the lower alloyed steel in high-temperature service, as a result of carbon migration. It is known that chromium and some other carbide-forming elements lower the chemical potential of carbon in steel, thus promoting carbon diffusion from the lower alloyed to the higher alloyed steel [2].

Influence of a decarbonized interlayer on the long-term strength of the joint has been the subject of discussions for many years. Most of the authors believe

that the interlayer has a noticeable influence on the mechanical properties [3–6]. In some works, however, no influence of the interlayer on creep fracture was reported [7]. The authors of all the published papers, however, agree in that the decarbonized interlayer has a lower hardness. The main difference in the opinions is related to fracture mode.

It is known from publications that there are two main types of creep damage accumulation processes that pertain to welded joints of low-alloy and high-alloy ferritic steels. One mode prevails at longer fracture time and lower loads, the other is prevalent at shorter time-to-fracture and higher loads. The first process is called cracking of type IV, and it is characterized by damage accumulation and crack initiation in the zone of normalizing temperatures and intercritical temperatures A_{C1} – A_{C3} in the HAZ. The other process is called cracking of IIIa type, and it is characterized by high local stresses and damage accumulation in the decarbonized interlayer in the HAZ near the fusion line [4].

The decarbonized interlayer is harmful for long-term strength of the welded joint not only because of formation of a microstructure, susceptible to microcracking, but also through localization of shear stresses and three-axial loads, in connection with the softness and higher ductility of the interlayer and high strength and lower ductility of the weld metal adjacent to the interlayer on the boundary with the base metal [8]. Dissolution of M_2C , M_7C_3 and $M_{23}C_6$ carbides within this area during the thermal cycle is also noted as an

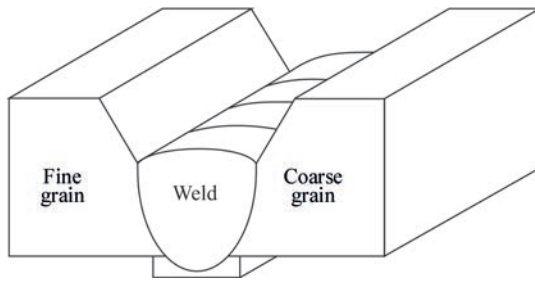


Figure 1. Scheme of welded joint with different grain size

additional factor for early destruction [9, 10]. In work [11] a statistical study on formation of cracks of type IV and IIIa was performed during inspection of power plants in Great Britain. The author came to the conclusion that a significant number of the defects were of IIIa type, and that carbon diffusion from low-alloy steels to high-alloy steels was the main cause for it.

As regards cracks of type IV, their formation is related to softening in the HAZ fine-grained zone and in the incomplete recrystallization zone (of intercritical temperatures A_{C1} – A_{C3}) [12]. One of the phenomena, accompanying the softening in these zones of low-alloy steels, is appearance of white etching interlayer (so-called white interlayer) [13, 14] at tempering and high-temperature service, which is formed by ferrite grains.

The objective of the work was revealing the features of inhomogeneity formation in the joints of dissimilar ferritic steels at tempering and an attempt to connect the phenomenon of formation of a decarbonized interlayer in the HAZ near-weld zone of low-al-

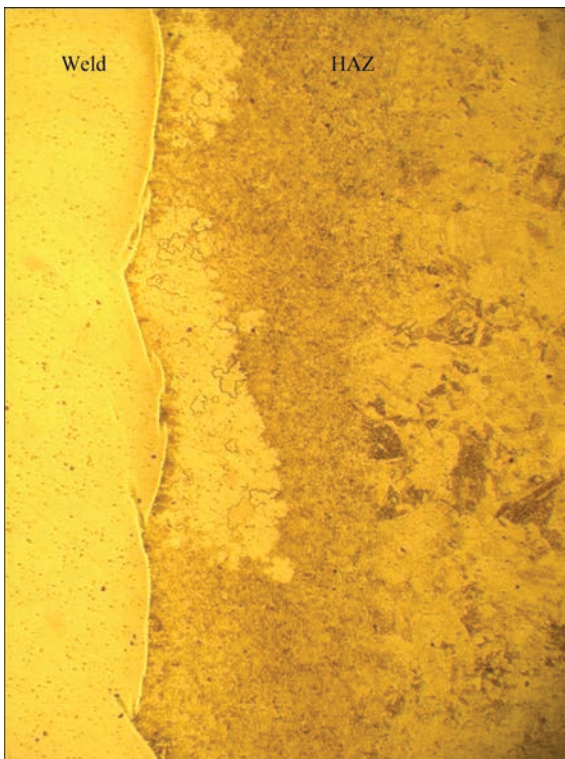


Figure 2. HAZ of multipass welds of P3 steel, welded by 9 % Cr electrodes, after tempering at 750 °C, for 8 h ($\times 25$ magnification)

loy steel in a combined multipass welded joint and of the white etching interlayer in the zone of normalizing and intercritical temperatures A_{C1} – A_{C3} .

Investigation procedure. Within the framework of microstructural studies of welded joints of 15Kh1M1F steel (reference designation P3; wt.%; 0.115 C; 0.648 Si; 0.67 Mn; 1.95 Cr; 0.16 Ni; 1.12 Mo; 0.32 V; 0.072 Nb; 0.15 Cu) with steels with 9 % Cr, experiments were conducted with the purpose of obtaining the structural inhomogeneity in the HAZ of the lower alloyed steel after high-temperature tempering, using different approaches to welding:

1) multipass welding of P3 steel with R91 steel using Thermanit Chromo 9V electrodes (wt.%; 0.09 C; 0.2 Si; 0.6 Mn; 9.0 Cr; 0.8 Ni; 1.1 Mo; 0.2 V; 0.05 Nb; 0.04 Ni) of 4 mm diameter, $I_w = 130$ – 135 A, $U_a = 24$ V; preheating and concurrent heating ~ 200 °C; higher welding speeds were used to produce beads of a small cross-section.

Welding was followed by tempering at 750 °C, for 8 h and 760 °C, for 4 h. Tempering at the temperatures of 750–760 °C was recommended both for R91 steel, Chromo 9V electrodes, and for P3 steel [14];

2) single-pass submerged-arc welding of P3 steel, using wire with 9 % Cr. The sides of the butt joints differed by the size of grains in the microstructure: one side of the butt joint, welded in as-delivered condition, had a fine-grained structure (grain size number $G = 9$ to DSTU EN ISO 643); the other side of the butt joint was subjected to prior heat treatment at 1200 °C, for 30 min (cooling in air) + 730 °C, for 3 h to obtain a coarse-grained structure (grain size number $G = 4$ to DSTU EN ISO 643). After that the joint was welded using Thermanit MTS 3 wire (wt.%; 0.1 C; 0.3 Si; 0.5 Mn; 9.0 Cr; 0.7 Ni; 1.0 Mo; 0.2 V) of 2.4 mm diameter with Bohler Marathon 543 flux in the following mode: $I_w = 360$ – 380 A, $U_a = 34.4$ V; $v_w = 20.7$ m/h (Figure 1).

For development of structural inhomogeneity welding was followed by tempering at the temperature of 750 °C, for 3 and 18 h.

3) deposition of two beads on PZ steel using Thermanit Chromo 9V electrodes of 3.2 mm diameter, $I_w = 115$ – 120 A, $U_a = 24$ V.

After deposition, tempering was performed at the temperature of 750 °C, for 3 and 18 h.

After welding and surfacing the templates were used to prepare microsections, which were photographed in the optical microscope, and hardness was measured.

In the first experiment, hardness was measured at 5 kg load in the weld and HAZ at the distance of ~ 0.3 , ~ 0.9 and ~ 1.4 mm from the fusion line. In the second experiment microhardness with 100 g load was measured for comparison on the joint sides with the fine and coarse grain. In the third experiment microhardness was

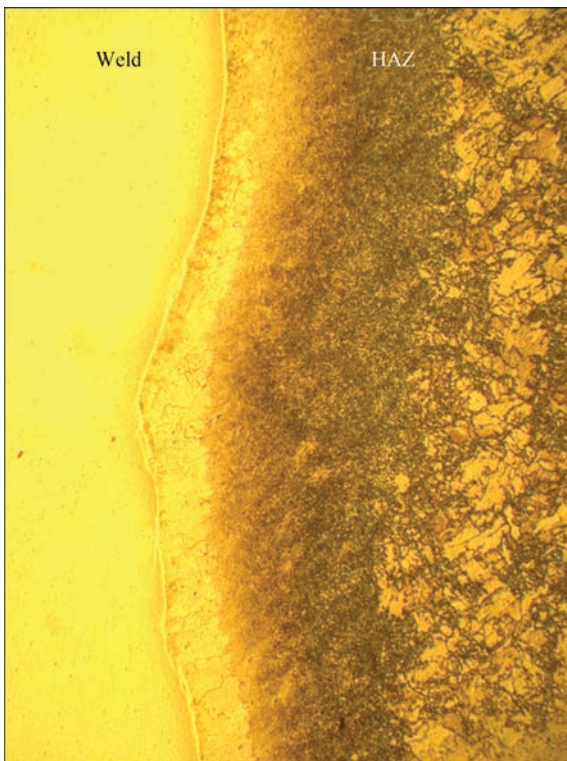


Figure 3. HAZ of multipass joints of P3 steel, welded by 9 % Cr electrodes, after tempering at 760 °C, for 4 h ($\times 25$ magnification)

measured with 100 g load, both in the section between the two beads, and under the middle of the second bead.

Experimental results and their analysis. In the first experiment after tempering at 750 °C, for 8 h and 760 °C, for 4 h formation of ferrite zones and ferrite interlayer is observed in the HAZ of P3 steel (Figures 2, 3). These interlayers form nonuniformly, and at a certain distance from the fusion line in some places (Figure 4), so that they cannot be directly related to carbon diffusion through the fusion surface. A characteristic feature of the microstructure in Figure 3 is presence of two interlayers in it: one in immediate vicinity of the fusion line, and the other, less pronounced, at a dis-

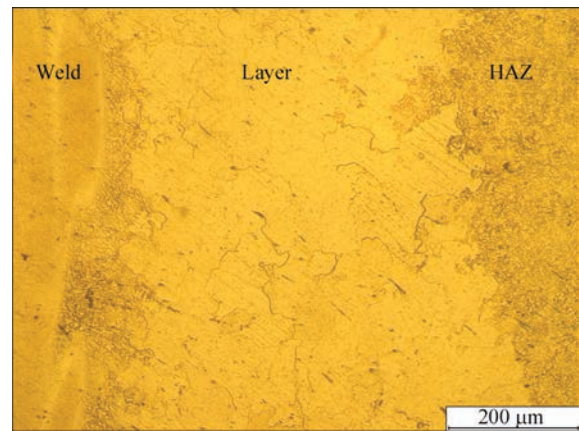


Figure 4. HAZ of multipass joints of P3 steel, welded by 9 % Cr electrodes, after tempering at 750 °C, for 8 h ($\times 160$ magnification) distance from the fusion line, approximately in the zone of intercritical temperatures $A_{C1}-A_{C3}$.

Both the micrographs, and hardness distribution (Figure 5) point to the fact that with temperature rise, the processes of structural inhomogeneity formation and softening in the near-weld zone begin to develop more rapidly in the HAZ of P3 steel.

In the second experiment in the joints of P3 steel with different grain size, a wide ferrite interlayer of a lower hardness (Figure 6) was observed in an area at a distance from the fusion line on the fine grain side after tempering at 750 °C for 18 h, while no such interlayer was found on the coarse grain side. Note that after tempering at 750 °C for 3 h, the interlayer was not observed on the fine grain side, either. The ferrite interlayer forms approximately in the HAZ fine grain zone, and in the zone that is heated during welding in $A_{C1}-A_{C3}$ temperature range. Variation of the interlayer width (it becomes wider on the top and at the bottom of the joint, near the butt surfaces) is attributable to considerable decarbonization of the surface, where the coefficient of carbon diffusion is the highest. Kinetics of ferrite interlayer formation is very well seen on thin single-pass samples after heat treatment (Fig-

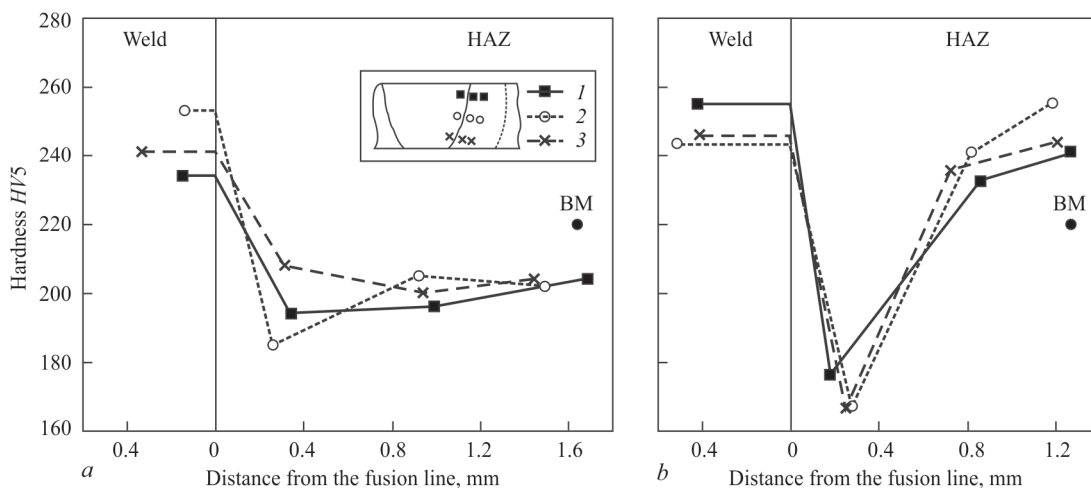


Figure 5. Hardness profile for the HAZ of multipass joints of P3 steel, welded with 9 % Cr electrodes, after tempering at 750 °C, for 8 h (a) and 760 °C, for 4 h (b)

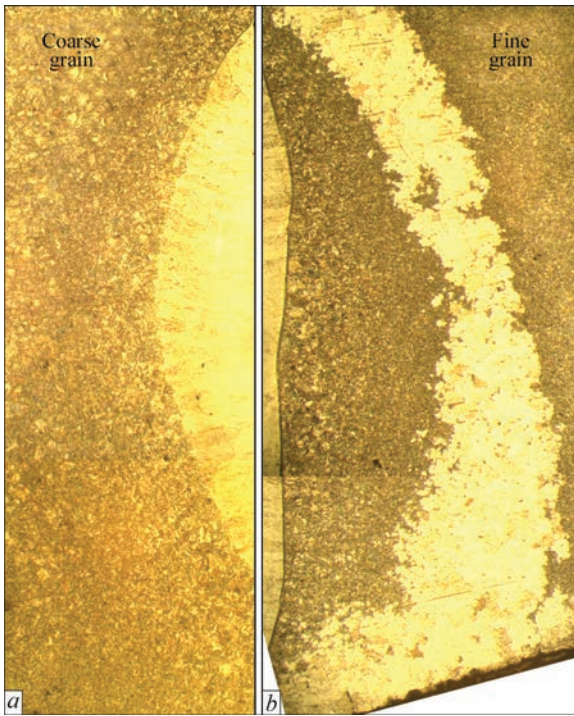


Figure 6. Microstructure of the HAZ of single-pass joint on P3steel with large $G = 4$ (a) and small $G = 9$ (b) initial grain size after tempering at 750 °C, for 18 h ($\times 25$ magnification)

ure 7). It is important to note that even in the case of thin samples decarbonization develops exactly along the fine grain zone of normalizing and intercritical temperatures.

Microhardness measurement on both sides of the butt joint also indicates softening in the ferrite interlayer (Figure 8). However, neither the panoramic photo of the microsection, nor the hardness profile demonstrate any noticeable decarbonization or softening in the near-weld zone near the fusion line, as in the case of multipass welding.

The main idea of the third experiment was simulation of the simplest variant of multipass welding, which would enable in each specific case determination of the factors, affecting formation of the ferrite interlayer in the near-weld zone of low-alloy steel HAZ.

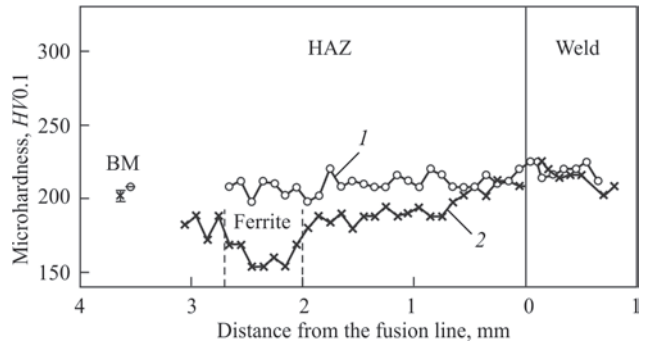


Figure 8. Microhardness measurement in a single-pass joint of P3 steel with different grain size after tempering at 750 °C for 18 h (1 — coarse grain; 2 — fine grain)

A characteristic feature of the HAZ structure in as-deposited condition is formation of fine-grain structure in the near-weld zone of the first bead that is located approximately in the normalizing zone and the intercritical zone from the second bead.

After soaking for 750 °C for 18 h, a ferrite area develops in this fine-grain zone of the first bead HAZ, formed at the second bead deposition. This area spreads perpendicular to the fusion line of the first bead, to the zone of normalizing and intercritical temperatures of the second bead (Figure 9). Similar results were obtained in work [15], where in a similar experiment decarbonization at tempering also began developing under the first bead through the zone of normalizing and intercritical temperatures from the second bead.

In the HAZ of P3 steel a drop in microhardness is observed in the intercritical temperature zone from the second bead after such a tempering, compared to microhardness under the second bead (Figure 10). Microhardness drop and formation of ferrite areas in the intercritical zone point to development of structural instability of this zone at high-temperature soaking. In other sections of deposition no ferrite areas or other structural inhomogeneities were reported.

These data point to the fact that the mechanism of the process of formation and development of the ferrite interlayer in the near-weld zone of the multi-

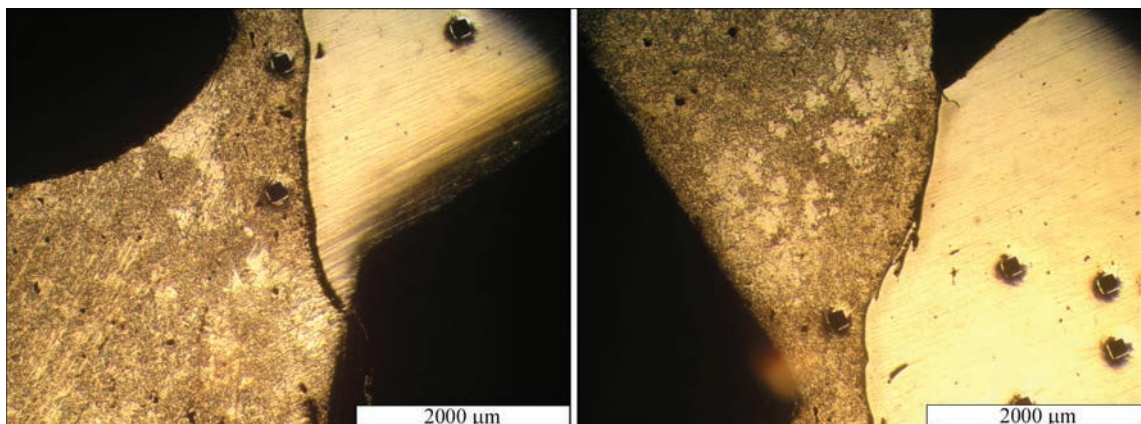


Figure 7. Single-pass joints of 15KH2M2FBS steel, welded with 9 % Cr electrodes, after tempering at 740 °C, for 4 h

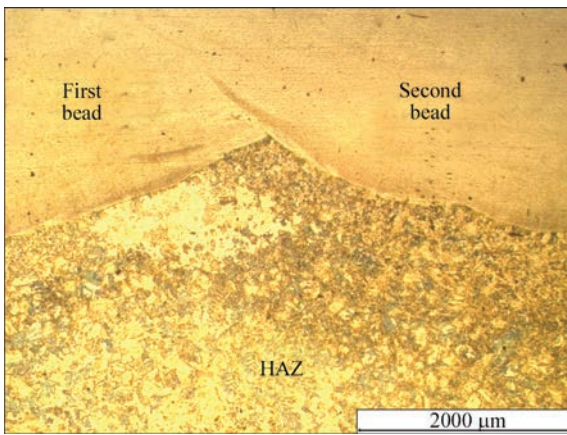


Figure 9. Microstructure of an area between the two beads at surfacing of 15Kh2M2FBS steel by 9 % Cr electrodes, after tempering at 750 °C, for 18 h ($\times 25$ magnification)

pass joint is similar to the process of formation and development of the white etching interlayer in the single-pass welded joint:

- in single-pass welded joint the role of diffusion intensifier was taken by the butt joint surfaces, which have a greater coefficient of diffusion, and where intensive decarbonization occurs (as a result of oxidation in the furnace atmosphere), whereas decarbonization developed in the fine-grain zone of normalizing and intercritical temperatures $A_{C1}-A_{C3}$ at a distance from the weld (Figures 6, 7);

- in a multipass welded joint the surface of fusion with the higher alloyed weld with a smaller chemical potential for carbon penetration, has the role of diffusion intensifier, while decarbonization developed in the fine-grain zone of normalizing and intercritical temperatures $A_{C1}-A_{C3}$ from the next beads, gradually covering the entire near-weld zone of the HAZ (Figure 11). Decarbonization can additionally develop in the vicinity of the intercritical zone at a distance from the weld (Figure 3).

This mechanism accounts for formation and development of ferrite areas near the fusion line in a multipass welded joint of R91+PZ steels. As was shown earlier, these ferrite areas in many places move away from the fusion line and develop in a less fine-grain zone at a slightly greater distance from the fusion line, making it impossible to explain this phenomenon by just the mechanism of direct diffusion from the near-weld zone into the weld. At multipass welding a complex superposition of the fields of temperature distribution from each of the beads develops in the near-weld zone of the low-alloy steel HAZ, both of those, which are directly superimposed on the base metal, and those, located in the second-third layer in-depth of the weld (Figure 11). This may result in development of a distribution of finer and coarser grains in the near-weld zone. The structure with the coarser grains has a smaller area of the grain bound-

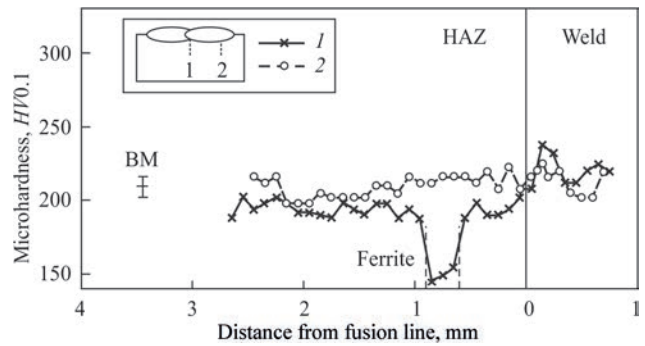


Figure 10. Microhardness measurement in a bead on 15Kh2M2FBS steel, deposited by 9 % Cr electrodes, after tempering at 750 °C, for 18 h

aries per a unit of volume. However, diffusion along the high-angle grain boundaries with their less densely-packed structure has the most important role at the temperatures of high-temperature tempering (up to the temperature of $0.6T_m$), compared to diffusion over dislocations and through the crystalline lattice [16]; in most cases the following ratio of the values of the coefficients of diffusion is realized in the metal volume:

$$D_{\text{lattice}} \ll D_{\text{dislocation}} \leq D_{\text{grain boundaries}} \leq D_{\text{surface}}$$

Therefore, reduction of the boundary area leads to lowering of the rate of carbon diffusion, and to lowering of the rate of decarbonized interlayer development, respectively, and vice versa.

This is exactly why the coarse-grain area in the near-weld zone directly at the fusion line in a multipass welded joint (Figure 4) has higher resistance to formation of structural inhomogeneity, unlike the normalizing zone, removed from the fusion line, through which the structural inhomogeneity develops (Figure 11). The same resistance to development of a «white interlayer» is demonstrated also by the side of the butt joint with initially coarse grain in the second experiment (Figure 6,

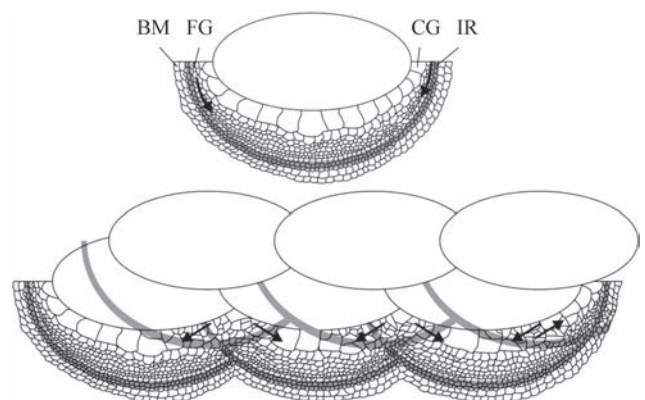


Figure 11. Superposition of intercritical zones in a multipass deposits and its comparison with a single-pass deposit: CG — coarse-grain HAZ; FG — fine-grain HAZ; IR — incomplete recrystallization zone (grey bands); BM — base metal; arrows show the direction of spreading of the decarbonized interlayer

a), in which the white etching interlayer does not develop even after tempering at 750 °C for 18 h.

These results allow noting the important role of the size of the grains in the processes of ferrite interlayer formation. It is envisaged that in the zones of normalizing and intercritical temperatures carbon fluctuation develops at high-temperature soaking, as a result of nonuniform distribution of carbon concentration in steel, fine grain sizes and high diffusion rates, respectively, and presence of surfaces with a higher coefficient of diffusion and lower chemical potential, leading to critical decarbonization and ferrite grain formation in some areas.

Additional factors, which may affect strength lowering in the incomplete recrystallization zone are [17]: 1) lath martensite transformation into subgrains with a low density of dislocations; 2) coagulation and coalescence of carbides (in particular, $M_{23}C_6$). Plastic deformation of the zone during tempering is mentioned as another reason for recrystallization and further growth of α -grains [13].

Figure 11 shows one of the examples of superposition of the temperature fields from the next beads. However, depending on the bead location and their orientation, a different distribution of the coarse and fine grains can form in the near-weld zone that may lead to another profile of decarbonization development in this zone.

Experimental results show that the white etching interlayer at a distance from the weld and the decarbonized interlayer in the HAZ near-weld zone of low-alloy steels, which develop in combined welded joints of dissimilar steels at tempering and in high-temperature service, can have the same mechanism of formation and propagation, and accordingly, the damages of IIIa and IV types in low-alloy steels operating in dissimilar steel joints at high temperatures can have the same initial cause: this is the influence of the thermal cycle of welding in the range of normalizing and incomplete recrystallization temperatures.

The main task, arising as a result of the study, is determination of the optimum geometrical configuration of surfacing or welding, at which the zones of normalizing and intercritical temperatures from the next beads at multipass welding will have the smallest specific length along the fusion line. For instance, in the case of deposition on surfaces of the same width, a compromise arises between making a smaller number of wider beads in the modes with a higher heat input that also have wider zones of normalizing and intercritical temperatures, and making a greater number of narrower beads, having narrower zones of normalizing and intercritical temperatures. It is assumed that in the first case wider individual ferrite accumulations will form (Figure 3), and in the second case a more uniform narrower interlayer will appear (Figure 4).

CONCLUSIONS

1. It is shown that zones with different decarbonization kinetics are observed in multipass welded joints of dissimilar ferritic steels after tempering, which was determined by the degree of microstructure etchability.

2. It was found that formation of white etching interlayer in the zone of normalizing and intercritical temperatures in the HAZ of pearlitic steels can depend on base metal grain size: the susceptibility to formation of a «white interlayer» in the incomplete recrystallization zone decreases with increase of the grain size.

3. It is shown that intensification of white etching interlayer formation can take place on the open surfaces of the butt joints.

4. It is also shown that at multipass welding of dissimilar steels intensification of formation of a decarbonized interlayer in the near-weld zone of the HAZ of lower alloyed steel occurs in the zones of normalizing and intercritical temperatures in the HAZ from the next beads.

5. It is noted that the phenomenon of development of a decarbonized interlayer near the fusion line can have a similar formation and propagation mechanism to that of the phenomenon of white etching interlayer formation in the zone of normalizing and intercritical temperatures.

REFERENCES

1. Di Gianfrancesco, A. (2017) *Materials for ultra-supercritical and advanced ultra-supercritical power plants*. Woodhead Publ.
2. DuPont, J.N. (2012) Microstructural evolution and high temperature failure of ferritic to austenitic dissimilar welds. *Int. Materials Reviews*, 57(4), 208–234.
3. Gotalsky, Yu.N. (1981) *Welding of dissimilar steels*. Kiev, Tekhnika [in Russian].
4. Helander, T., Andersson, H. C. M., Oskarsson, M. (2000) Structural changes in 12–2.25 % Cr weldments — an experimental and theoretical approach. *Materials at High Temperatures*, 17(3), 389–396.
5. Zhao, Y., Gong, J., Wang, X. et al. (2015) Carbon diffusion in dissimilar joints between P91 and 12Cr1MoV steels welded by different consumables at high temperature. *Ibid.*, 32(6), 557–565.
6. Khromchenko, F.A. (2010) *Peculiarities and causes of damages of pipeline welded joints (Background materials)*. Moscow, STC Energoprogress [in Russian].
7. Jandová, D., Kasl, J., Kanta, V. (2006) Creep resistance of similar and dissimilar weld joints of P91 steel. *Materials at High Temperatures*, 23(3–4), 165–170.
8. Mayr, P., Schlacher, C., Siefert, J. A., Parker, J. D. (2018) Microstructural features, mechanical properties and high temperature failures of ferritic to ferritic dissimilar welds. *Int. Materials Reviews*, 64(1), 1–26.
9. Dawson, K. E., Tatlock, G. J., Chi, K., Barnard, P. (2013) Changes in precipitate distributions and the microstructural evolution of P24/P91 dissimilar metal welds during PWHT. *Metallurgical and Materials Transact. A*, 44, 5065–5080.
10. Laha, K., Chandravathi, K.S., Bhanu Sankara Rao, K. et al. (2001) An assessment of creep deformation and fracture

- behavior of 2.25Cr–1Mo similar and dissimilar weld joints. *Ibid.*, **32**, 115–124.
11. Brett, S.J. (2004) Type IIIa cracking in 1/2CrMoV steam pipe-work systems. *Sci. and Technol. of Welding and Joining*, **9**(1), 41–45.
 12. Cerjak, H., Mayr, P. (2008) *Creep strength of welded joints of ferritic steels*. In: *Creep-resistant steels*. Ed. by F. Abe, T.-U. Kern, R. Viswanathan. Woodhead Publ.
 13. Hrivnak, I., Malinovska, E., Mosny, Ya. (1983) To problem of formation of «white layer» in narrow-gap submerged arc welding. *VUZ*, **XIX**, **1**.
 14. German, S.I. (1972) *Electric arc welding of heat-resistant steels of pearlite class*. Moscow, Mashinostroenie [in Russian].
 15. Lundin, C.D., Khan, K.K., Yang, D. (1995) Effect of carbon migration in Cr–Mo weldments on metallurgical structure and mechanical properties. *Welding Research Council Bulletin*, **407**, 1–49.
 16. Mehrer, H. (2007) *Diffusion in Solids. Fundamentals, Methods, Materials, Diffusion-Controlled Processes*. Springer-Verlag.
 17. Laha, K., Chandravathi, K.S., Parameswaran, P. et al. (2007) Characterization of microstructures across the heat-affected zone of the modified 9Cr–1Mo weld joint to understand its role in promoting type IV cracking. *Metallurgical and Materials Transact. A*, **38**, 58–67.

ORCID

M.O. Nimko: 0000-0002-9672-4921,
V.Yu. Skulskyi: 0000-0002-4766-5355

CONFLICT OF INTEREST

The Authors declare no conflict of interest

CORRESPONDING AUTHOR

V.Yu. Skulskyi
E.O. Paton Electric Welding Institute of the NASU
11 Kazymyr Malevych Str., 03150, Kyiv, Ukraine
E-mail: vsku@paton.kiev.ua

SUGGESTED CITATION

M.O. Nimko, V.Yu. Skulskyi, A.R. Gavryk,
S.I. Moravetskyi and I.G. Osypenko (2021) Structural inhomogeneity in welded joints of heat-resistant steels of chromium-molybdenum-vanadium system with different chromium content. *The Paton Welding J.*, **10**, 11–17.

JOURNAL HOME PAGE

<https://pwj.com.ua/en>

Received 22.07.2021
Accepted: 11.11.2021